HHS Public Access

Author manuscript

Proteins. Author manuscript; available in PMC 2018 February 16.

Published in final edited form as:

Proteins. 2010 February 15; 78(3): 714–722. doi:10.1002/prot.22604.

Characterization of intrinsically disordered proteins with electrospray ionization mass spectrometry: conformational heterogeneity of α-synuclein

Agya K. Frimpong[1], **Rinat R. Abzalimov**[1], **Vladimir N. Uversky**[2,3], and **Igor A. Kaltashov**[1,✉]

[1]Department of Chemistry, University of Massachusetts Amherst, Amherst, MA

[2]Institute for Intrinsically Disordered Protein Research, Center for Computational Biology and Bioinformatics, Indiana University School of Medicine, Indianapolis, IN

[3]Institute for Biological Instrumentation, Russian Academy of Sciences, Pushkino, Russia

Abstract

Conformational heterogeneity of α-synuclein was studied with electrospray ionization mass spectrometry by analyzing protein ion charge state distributions, where the extent of multiple charging reflects compactness of the protein conformations in solution. While α-synuclein lacks a single well-defined structure under physiological conditions, it was found to sample four distinct conformational states, ranging from a highly structured one to a random coil. The compact highly structured state of α-synuclein is present across the entire range of conditions tested (pH ranging from 2.5 to 10, alcohol content from 0 to 60%), but is particularly abundant in acidic solutions. The only other protein state populated in acidic solutions is a partially folded intermediate state lacking stable tertiary structure. Another, more compact intermediate state is induced by significant amounts of ethanol used as a co-solvent and appears to represent a partially folded conformation with high β-sheet content. Protein dimerization is observed throughout the entire range of conditions tested, although only acidic solutions favor formation of highly structured dimers of α-synuclein. These dimers are likely to present the earliest stages in protein aggregation leading to globular oligomers and, subsequently, protofibrils.

Keywords

protein conformation; intrinsic disorder; mass spectrometry; electrospray ionization; charge state distribution; α-synuclein; aggregation; amyloidosis

Introduction

Until recently, a well-defined protein structure was considered an absolute requirement for its biological function and the lack of stable conformation always had a negative

✉Address correspondence to: Igor A. Kaltashov, Department of Chemistry, University of Massachusetts-Amherst, 701 North Pleasant Street, Lederle Graduate Research Tower 701, Amherst, MA 01003, Tel (413) 545-1460, Fax (413) 545-4490, Kaltashov@chem.umass.edu.

Supporting Information: Details of chemometric processing of the set of α-synuclein ESI MS data

connotation, as unstructured proteins were viewed as unstable species lacking any functional activity and prone to aggregation. The limitations of this view are now becoming apparent, following the realization that that the intrinsic disorder (*i.e.*, high flexibility exhibited under native conditions) not only is quite ubiquitous in nature, but is in fact vital for the function of many proteins (1-8). A paradigm shift in our viewing of large-scale dynamics as a defining element of protein function places a premium on the ability to characterize non-native states (both transiently populated and intrinsically disordered). Theoretical prediction of properties of disordered proteins is usually based on the assumption that they lack any structure in solution, which allows utilization of well-established theories of polymer physics in their description (9). The major deficiency of this approach is its neglect of any residual structure, which often exists in denatured protein states (10-15). Furthermore, co-existence of several protein states in solution at equilibrium makes even their detection an extremely challenging experimental task for established biophysical techniques (16).

Electrospray mass spectrometry (ESI MS) has recently emerged as a powerful alternative tool capable of both detection and characterization of non-native protein states under a variety of conditions (17). It offers several important advantages, which make it a very attractive tool to probe structure and dynamics of biopolymers. One particularly important advantage of ESI MS is its ability to make a distinction between various conformations based on the extent of multiple charging of protein ions, whose appearance is determined by the protein tertiary structure (18). Tightly folded proteins undergo ESI to give ions carrying a relatively small number of charges, as their compact shape in solution does not allow a significant number of protons to be accommodated on the surface upon transition to the gas phase. On the contrary, less structured protein conformers give rise to ions carrying a significantly larger number of charges, as many more protons can be accommodated on the surface of a protein once it loses its compactness. If both native and denatured states of the protein co-exist at equilibrium in solution, the protein charge-state distributions are bimodal. Dramatic changes of protein charge-state distributions often serve as gauges of large-scale conformational changes (19). This feature is widely used to study protein dynamics in processes ranging from folding (20-22) and non-enzymatic post-translational modifications (23) to ligand binding (24-27), protein assembly (28-30), and protein interaction with other biopolymers (31, 32).

In this work we apply ESI MS to probe higher order structure of α-synuclein, a neuronal protein which is believed to play a major role in development of Parkinson's disease (33-36), although its normal biological function remains a subject of debate (37). While α-synuclein lacks a well-defined three-dimensional structure in solution, available spectroscopic evidence indicates that it may adopt a series of different conformations depending on its environment or co-factors (38). In this work we use ESI MS to show that four different conformations of α-synuclein co-exist in solution under equilibrium, which differ from each other very significantly by the degree of compactness. One of these conformations (whose abundance reaches maximum under acidic conditions) appears to be tightly folded. Correlating the abundance evolution of these conformers as a function of pH with the earlier spectroscopic measurements allows conclusions to be made regarding the nature of these states. In addition to the monomeric α-synuclein, two types of dimers are observed, whose relevance for protein aggregation is discussed.

Materials and Methods

Materials

Human recombinant α-synuclein was expressed in *E. coli* and purified as described previously (39). Following purification, the protein was dialyzed four times against de-ionized water at 4°C, lyophilized and stored at –80°C. Stock solutions of α-synuclein were diluted to a level of 10 μM (unless specified otherwise) in a 10 mM ammonium acetate solution, whose pH was adjusted to a desired level using either acetic acid or ammonium hydroxide, followed by pH re-measurement of the final protein solutions prior to MS analysis. All chemicals were of analytical grade or higher.

Mass Spectrometry

Charge state distribution analysis of α-synuclein ions was based upon ESI mass spectra acquired with a JMS-700 MStation (Tokyo, Japan) two-sector mass spectrometer equipped with a standard ESI source. Protein solutions were continuously infused into the ESI source at a flow rate of 3 μL/min. ESI source settings were kept constant throughout the measurements to minimize variability of ionic charge state distributions caused by changing instrumental parameters. All mass spectra were acquired by scanning the magnet at a rate of 5 s/decade. Typically, 200 scans were averaged to record each spectrum in order to ensure a high signal-to-noise ratio. The ionic intensities of various charge state distributions were arranged as a $K \times N$ matrix, where each column represented one of the N mass spectra measured under certain conditions and each row represented one of the K charge states used in the analysis. Since each charge state z was represented in mass spectra by an envelope of closely spaced peaks corresponding to $[M + (z\text{-}m)H + mNH_4]^{z+}$ ions, the ionic intensities were calculated as areas of such envelopes. Chemometric processing of ESI mass spectra was carried out using Origin 6.0 software package (Microcal Software, Inc., Northampton, MA) as described previously (40).

Fragmentation of α-synuclein dimer ions was carried out on a QSTAR-XL (Applied Biosystems/MDS-Sciex, Toronto, Canada) hybrid quadrupole/time-of-flight mass spectrometer (QqTOF MS) equipped with a TurboSpray ion source. The precursor ions were mass-selected in the quadrupole mass analyzer (Q) and subjected to collision-induced dissociation (CAD) in the RF-only quadrupole (q), followed by detection of all resulting fragment ions in the time-of-flight (TOF) mass analyzer.

Results

ESI mass spectra of α-synuclein acquired at neutral pH display a convoluted charge state distribution for monomeric protein ions ranging from +6 to +22 (Figure 1). High charge density protein ion peaks are prominent in all spectra, including those acquired at near-neutral pH, consistent with the notion of the extent of multiple charging in ESI MS reflecting the degree of compactness of the polypeptide chain in solution (18, 41). It is important to note, however, that low charge density protein ions (charge states + 7 through +9) are also present in the spectra at near-neutral pH. Relative contribution of these ions to the overall ionic signal becomes particularly significant at low pH (*e.g.*, top panel on Figure

1). A close inspection of mass spectra strongly suggests that in addition to the low charge density component of the ionic signal, at least two distinct components are present in the high charge density parts of mass spectra. The first one is an envelope of ion peaks around charge state +14, and the second group is clustered around charge state +19. The relative abundance of ionic species representing these two groups does not change in concert, particularly under acidic conditions. Indeed, while both groups become significantly less populated at pH 2.5 compared to the low charge density ionic species, the highest charge density ions (clustered around +19) are diminished to a much greater extent (Figure 1, top trace).

Presence of ethanol as a co-solvent at low levels (20% by volume) did not dramatically change the appearance of α-synuclein ions charge state distributions in ESI MS (Figure 2). However, increasing the ethanol content to 60% by volume resulted in a noticeable change in the ionic charge state distribution: +10 and +11 ions, whose peaks previously formed a visible minimum in the distribution, now become highly populated. This feature was absent in the mass spectrum of α-synuclein acquired in the presence of TFE (either 20% or 60%, data not shown).

To determine the number of independent components giving rise to the observed variance of the charge state distributions of α-synuclein monomers, the entire set of experimental data (an 18×8 matrix) was subjected to a singular value decomposition (SVD), which yielded four significant singular values (see Supporting Information for more detail). The results of deconvolution of charge state distributions of α-synuclein ions by finding the optimal fit for the entire data set with four basis functions are shown in Figures 3 and 4. Each basis function was selected as a symmetric (Gaussian) curve, whose parameters (position of the maximum and width, see Table 1) were maintained nearly constant through the entire set of charge state distributions, while its relative abundance was allowed to change from one spectrum to another without any constraints. The lowest charge density basis function represents the most compact conformer of α-synuclein (labeled ***C*** in Figures 3 and 4). Its solvent-accessible surface area was estimated to be 7.3×10^3 Å^2 based on the average ionic charge using the approach developed in our laboratory for folded proteins (42). The highest charge-density basis function is likely to represent mostly unstructured protein (labeled ***U*** in Figures 3 and 4). The charge density ratio for these two conformers is $Z_U/Z_C = 2.2$. Two other basis functions (labeled I_1 and I_2 in Figures 3 and 4) represent intermediate levels of charge density.

A distinct feature of α-synuclein ion charge state distributions is that all four basis functions are needed to reconstruct the total ionic signal in all but one acquired spectra. The exception is the mass spectrum acquired at pH 2.5, where only two basis functions are needed in order to restore the overall appearance of the ionic charge state distribution. Another peculiar feature worth mentioning here is the presence of the ionic signal corresponding to the compact conformer ***C*** in all spectra acquired in this work, although its relative contribution to the overall ionic signal is the highest under acidic conditions. Another conformer, which appears to be populated under all conditions tested, is an intermediate state I_1. The high charge-density component of the ionic signal (unstructured state, ***U***) is negligible at low pH, but becomes prominent as the solution pH is increased. It becomes suppressed at high pH

when a large amount of ethanol (but not TFE) is used as a co-solvent. Ionic contribution of I_2 to the total ion current remains modest under most conditions tested (it actually is absent at pH 2.5), but becomes prominent in the presence of large amounts of ethanol.

In addition to the monomeric ions, the ESI mass spectra of α-synuclein also contain contributions from non-covalently bound protein dimers. Interestingly, the extent of multiple charging of protein dimers depends on the solution pH: the mass spectra acquired at pH 2.5 feature a narrow distribution of dimeric species clustered around charge state +11, while the spectra acquired at pH 4 and above display a wide distribution of dimer ions at higher charge states (+13 through +26). In order to establish the nature of the non-covalent dimers, two representative dimer ions were mass-selected in the quadrupole mass analyzer (Q) of a hybrid QqTOF mass spectrometer and subjected to collision-activated dissociation (CAD) in the RF-only quadrupole (q), followed by detection of all resulting fragment ions in the time-of-flight (TOF) mass analyzer.

Figure 5A shows the mass spectrum of fragment ions generated by CAD of a +17 dimer ion (solution pH 8). The dissociation event gives rise to pairs of monomers with a relatively narrow and symmetric charge state distribution. There are two most abundant pairs of complementary fragments, which together account for over 98% of the entire ionic signal, namely +8/+9 and +7/+10. There is no evidence in the spectrum for the asymmetric charge partitioning, typical for dissociation of non-covalent dimers and higher oligomers composed of folded monomers (43, 44). Similar results were obtained for the dissociation of several other high charge density dimer ions (data not shown). Unlike fragmentation of high charge density dimers of α-synuclein, dissociation of dimers carrying fewer charges clearly proceeds via the so-called asymmetric charge partitioning mechanism. Collisional activation of a +11 dimer of α-synuclein generated by ESI at pH 2.5 gives rise almost exclusively to a +7/+4 complementary pair of monomers, with a minor contribution from the +6/+5 pair (Figure 5B).

Discussion

The emergence of the notion of intrinsic disorder several years ago changed the discourse in structural biology by challenging one of its central paradigms, which linked functional competence to a well-defined structure. The lack of such structure had a negative connotation, as non-native proteins were traditionally viewed as unstable species lacking any functional activity and prone to aggregation. It now becomes clear that this view needs to be modified, as a growing number of proteins are found to be either partially or fully unstructured under native conditions, both *in vitro* and *in vivo* (45). Although the intrinsic disorder is quite ubiquitous in nature and is vital for the function of many proteins, it is important to realize that a delicate balance between order and chaos must be maintained in order to ensure the proper functioning and indeed the very survival of a cell. Protein misfolding is implicated in a variety of pathological conditions, most notably those related to amyloidosis, such as Alzheimer's disease (46-49).

α-Synuclein is a neuronal protein, whose notorious lack of well-defined higher order structure made it a paradigmatic member of the growing family of intrinsically unstructured

proteins (38). Although the physiological function of α-synuclein remains a subject of an on-going inquiry, it has been identified as a major component of Lewy bodies, a neuropathological hallmark of Parkinson's disease (33, 50). α-Synuclein is also a component of proteinaceous inclusions typical of several other neurodegenerative diseases collectively known as synucleinopathies (33, 34, 51). While being commonly referred to as "unstructured," α-synuclein has physical dimensions below those expected for a completely unstructured random coil (38) and demonstrates contact rates among distant residues that indicate much shorter separation than is expected for a random polymer chain (52). Conformational heterogeneity of α-synuclein in solution is strongly suggested by the results of a recent study utilizing non-covalent labeling of proteins prior to ESI MS (53). Spectroscopic measurements also reveal the ability of α-synuclein to display a range of different conformational signatures *in vitro* depending on its environment, post-translational modifications and presence of binding partners (38). Of particular interest is the ability of α-synuclein to display dramatic changes of secondary structure and its propensity to form aggregates as a result of changing solution pH and/or organic co-solvent content. So far, detailed structural characterization of α-synuclein has been possible only in the presence of stabilizing micelles (54), although the helical structures adopted by the protein under such conditions were proposed to exist even in the absence of micelle or membrane binding (55).

Earlier circular dichroism (CD) measurements indicated that in acidic solutions α-synuclein adopts a *partially folded conformation* with significant helical content (38). Protein ion charge state distributions in ESI mass spectra acquired at pH 2.5 (Figures 1 and 3) suggest that α-synuclein populates mostly two states under these conditions, one of which is compact. While this compact state (labeled ***C*** in Figure 3) appears to be highly structured (*vide infra*), the second, less compact state (labeled $\boldsymbol{I}_1$ in Figure 3) is also likely to retain some structure, as it is very distinct from the unstructured state of the protein. The latter (labeled ***U*** in Figure 3) becomes populated at pH ≥ 4, and its ionic signal is more prominent in basic solutions. Another distinct state, which is notably absent under the strongly acidic conditions and becomes prominent in the presence of ethanol as co-solvent (labeled $\boldsymbol{I}_2$ in Figure 3), is even more compact than $\boldsymbol{I}_1$, as judged by the charge density of corresponding ions in ESI MS.

Given the conclusions of the previous studies of α-synuclein behavior in solution (38), it is not very surprising that two distinct semi-compact, intermediate state exists in solution over a range of conditions. What is surprising, however, is the fact that protein ion charge state distributions in all of the collected spectra contain a contribution from a very compact state ***C*** (it should be mentioned that the fractional concentration of this state in solution may be even higher than suggested by the relative abundance of the ionic signal of ***C***, as the ESI process may discriminate against it and favor higher charge-density protein ions under our experimental conditions (56)). The ionic contribution to the total ion signal is very distinct and its detection does not even require chemometric processing of the data. Usually this is a unique feature of natively folded (18, 40, 57) or highly structured non-native (58) protein conformations. It is very unusual for the low charge-density protein ions to dominate ESI MS at strongly acidic pH, since it typically favors protein unfolding (a notable exception is pepsin (19, 44), whose "native" environment is highly acidic). However, the existence of a

compact conformation of α-synuclein and its prominence at low pH is consistent with the conclusions of recent studies that used negative ion ESI MS and ion mobility spectroscopy to investigate early stages of aggregation of this protein (59, 60).

α-Synuclein is believed to lack a folded state, although a recent work suggests that it may have an intrinsic propensity for adopting at least two helical structures, one of which is mostly folded (54, 55). Furthermore, measurements of gas phase collisional cross-sections of low charge density polyanions of α-synuclein carried out using ion mobility spectroscopy were consistent with the globular conformation of this protein in the solvent-free environment (60), although it remains unclear whether the hydrophobic collapse could be a significant factor influencing the outcome of these measurements. In order to provide quantitative evidence that the detected compact state ***C*** does indeed represent a highly structured conformer of α-synuclein, we analyzed the difference in the extent of multiple charging between a natively folded conformation and a random coil state for several well-characterized proteins. The graph in Figure 6 shows the ratios of average charges of ions representing native conformers (Z_N) and fully unstructured polypeptide chains (Z_U) for a set of proteins whose conformational dynamics was analyzed previously in our laboratory. This set includes chymotrypsin inhibitor II, ubiquitin (40), cellular retinoic acid binding protein I, myoglobin (57) and pepsin (44).

According to a current view of ESI process, the extent of multiple charging of natively folded proteins Z_N is determined by their solvent-accessible surface area (42, 61), while the number of charges accumulated by a random coil Z_U depends on the chain length (41). As a first order approximation, surface of a folded protein and the chain length can be linked to each other by assuming that a folded protein is a sphere of radius R and uniform density ρ_o, which has the same mass as a chain L with a uniform linear density ρ_γ:

$$\frac{4}{3}\pi R^3 \cdot \rho_o = L_{\rho_\gamma}. \quad (1)$$

In this case the ratio of the chain length to the surface of the sphere S will be

$$\frac{L}{S} = \left(\frac{\rho_o}{12\pi^2\rho_\gamma}\right)^{2/3} \cdot L^{1/3}, \quad (2)$$

and, therefore, the Z_U/Z_N ratio should depend upon the polypeptide chain length as

$$\frac{Z_U}{Z_N} = A \cdot L^{1/3}. \quad (3)$$

Since in our approximation linear density is uniform, Z_U/Z_N can be expressed in terms of the protein molecular weight, rather than the chain length L:

$$\frac{Z_U}{Z_N} = \boldsymbol{B} \cdot \sqrt[3]{MW}, \quad (4)$$

and the ratio of Z_U/Z_N to $(\mathrm{MW})^{1/3}$ is expected to be constant.

The Z_U/Z_N to $(\mathrm{MW})^{1/3}$ ratio for the five model "foldable" proteins is indeed nearly constant (see Figure 6), suggesting that the approximations made to derive expressions (3) and (4) are reasonable. Importantly, the Z_U/Z_C ratio for α-synuclein fits this curve, suggesting that the two states populated in acidic solution do indeed represent a random coil (***U***) and a highly structured conformation (***C***). Although the actual higher order structure of the ***C*** state is yet to be determined, the appearance of a far-UV CD spectrum of α-synuclein in acidic solutions reveals a significant α-helical content. It is reasonable to assume that both equilibrium states co-existing in solution at low pH (***C*** and $\boldsymbol{I}_1$) have significant α-helical secondary structure, but the tertiary contacts are present only in ***C***, while the greatly diminished compactness of $\boldsymbol{I}_1$ likely suggests that it lacks a stable tertiary structure and may in fact resemble a micelle-bound helical form of α-synuclein (54).

Identification of another intermediate state of α-synuclein, $\boldsymbol{I}_2$, is aided by the fact that its contribution to the total ion signal remains very modest unless high concentration ethanol is used as a co-solvent, the conditions leading to an apparent increase of the β-sheet content as suggested by the results of both CD (38) and Raman spectroscopic measurements (62). It is, therefore, reasonable to assume that the $\boldsymbol{I}_2$ intermediate contains segments folded as β-strands. Furthermore, a relatively modest extent of multiple charging displayed by this intermediate state indicates that it is more compact compared to $\boldsymbol{I}_1$, consistent with the notion of the tertiary structure of $\boldsymbol{I}_2$ defined by inter-strand contacts and a lack of tertiary contacts in the $\boldsymbol{I}_1$. On the other hand, a slightly higher extent of multiple charging of $\boldsymbol{I}_2$ compared to ***C*** is likely to indicate that some protein segments fail to adopt a well-defined structure. A recent study of α-synuclein amyloids by H/D exchange revealed significant protection within the continuous middle segment of the protein spanning residues 39-101, some protection in the N-terminal segment and no protection in the C-terminal segment (63). It is possible that the increased propensity of the middle segment of α-synuclein to adopt β-stranded conformation may result in formation of β-structure within protein monomers as well when assisted by such secondary structure inducer as ethanol. At the same time, diminished β-propensity in the C-terminal segment and, at least to some extent, in the N-terminal segment prevents folding of the entire chain, making $\boldsymbol{I}_2$ a partially unstructured state.

A very interesting question that arises in connection with considering various conformations of α-synuclein detected by ESI MS is their relevance for the fibrillation process. Although the measurement time scale and protein concentrations used in our work were unlikely to cause fibril formation, ESI MS reveals the presence of α-synuclein dimers across the entire

range of solution conditions tested in this work. Intriguingly, at least two different types of dimers are observed, which can be distinguished based on the extent of multiple charging of corresponding ions in ESI mass spectra. Only low charge density dimer ions are observed under acidic conditions, while increasing the solution pH to 4 and above favors formation of high charge density dimer ions. The dissociation behavior of homodimers depends on their solution-phase structure (64), and the asymmetric charge partitioning accompanying dissociation of low charge density dimer ions (Figure 5) provides a clear indication that they are composed of highly structured monomers. On the other hand, asymmetric charge partitioning is not observed for dissociation of dimer ions at higher charge states, clearly suggesting that both monomeric constituents of such dimers are mostly unstructured.

Intriguingly, the conditions that favor formation of structured helical monomers and dimers of α-synuclein also result in fastest protein fibrillation (38). While this may seem contradictory to the fact that amyloid fibrils have cross-β-structure (65), recent studies of α-synuclein oligomerization by atomic force microscopy and Raman spectroscopy revealed the globular character of early stage oligomers (66). These spheroidal oligomers had significant helical content (nearly 50%), which decreases to about 37% in protofilaments. Furthermore, a recent thermodynamic analysis of α-synuclein conformational dynamics also provided evidence that a highly structured helical state populated at low pH is a pre-requisite for protein aggregation (55). Finally, the results of a recent ion mobility spectroscopy study suggest that α-synuclein aggregation is facilitated when the conformational ensemble is biased towards compact (“collapsed”) conformation(s) (59). Therefore, it is not unreasonable to assume that the compact dimeric species observed in acidic solutions are early precursors to the globular oligomers, although the validity of this conjecture must be carefully investigated, a task that lies outside of the scope of this work. Finally, larger α-synuclein oligomers whose presence in solution can be detected by methods of atomic force microscopy (66) or optical spectroscopy (67) presently remain out of reach of mass spectrometry, rapid progress in characterization of large macromolecular complexes by ESI MS (61, 68) is likely to make such measurements possible in a not-so-distant future.

Conclusions

We demonstrated that α-synuclein populates four distinct conformational states, ranging from a highly structured one to a random coil, the former being present across the entire range of conditions tested (pH ranging from 2.5 to 10, alcohol content from 0 to 60%), but being particularly abundant in acidic solutions. The two intermediates are identified as less compact helical and more compact β- rich states, the latter being induced by significant amounts of ethanol used as a co-solvent. Acidic conditions also favor formation of highly structured dimers of α-synuclein, which appear to represent the earliest stages in protein aggregation leading to globular oligomers and, subsequently, protofibrils. This work also demonstrates the enormous potential of ESI MS for characterization of conformational dynamics of intrinsically unstructured proteins.

Supplementary Material

Refer to Web version on PubMed Central for supplementary material.

Acknowledgments

This work was supported by grants CHE-0406302 and CHE-0750389 from the National Science Foundation (I.K.), R01 LM007688-01A1 and GM071714-01A2 from the National Institutes of Health (V.N.U.) and by the Program of the Russian Academy of Sciences for the “Molecular and cellular biology” (V.N.U.). The authors gratefully acknowledge the support of the IUPUI Signature Centers Initiative.

References

1. Romero P, Obradovic Z, Kissinger CR, Villafranca JE, Garner E, Guilliot S, Dunker AK. Thousands of proteins likely to have long disordered regions. Pac Symp Biocomput. 1998; 3:437–448.
2. Wright PE, Dyson HJ. Intrinsically unstructured proteins: re-assessing the protein structure-function paradigm. J Mol Biol. 1999; 293:321–331. [PubMed: 10550212]
3. Uversky VN, Gillespie JR, Fink AL. Why are “natively unfolded” proteins unstructured under physiologic conditions? Proteins: Structure, Function, and Genetics. 2000; 41:415–427.
4. Tompa P. Intrinsically unstructured proteins. Trends Biochem Sci. 2002; 27:527–533. [PubMed: 12368089]
5. Dyson HJ, Wright PE. Intrinsically unstructured proteins and their functions. Nat Rev Mol Cell Biol. 2005; 6:197–208. [PubMed: 15738986]
6. Xie H, Vucetic S, Iakoucheva LM, Oldfield CJ, Dunker AK, Uversky VN, Obradovic Z. Functional anthology of intrinsic disorder 1 Biological processes and functions of proteins with long disordered regions. J Proteome Res. 2007; 6:1882–1898. [PubMed: 17391014]
7. Uversky VN, Dunker AK. Biochemistry: Controlled Chaos. Science. 2008; 322:1340–1341. [PubMed: 19039128]
8. Dunker AK, Oldfield C, Meng J, Romero P, Yang J, Chen J, Vacic V, Obradovic Z, Uversky V. The unfoldomics decade: an update on intrinsically disordered proteins. BMC Genomics. 2008; 9:S1.
9. Bright JN, Woolf TB, Hoh JH. Predicting properties of intrinsically unstructured proteins. Progr Biophys Mol Biol. 2001; 76:131–173.
10. Shortle D. The denatured state (the other half of the folding equation) and its role in protein stability. FASEB J. 1996; 10:27–34. [PubMed: 8566543]
11. Smith LJ, Fiebig KM, Schwalbe H, Dobson CM. The concept of a random coil Residual structure in peptides and denatured proteins. Fold Des. 1996; 1:R95–R106. [PubMed: 9080177]
12. Blanco FJ, Serrano L, Forman-Kay JD. High populations of non-native structures in the denatured state are compatible with the formation of the native folded state. J Mol Biol. 1998; 284:1153–1164. [PubMed: 9837733]
13. Hammarstrom P, Carlsson U. Is the unfolded state the Rosetta Stone of the protein folding problem? Biochem Biophys Res Comm. 2000; 276:393–398. [PubMed: 11027486]
14. Shortle D. The expanded denatured state: an ensemble of conformations trapped in a locally encoded topological space. Adv Protein Chem. 2002; 62:1–23. [PubMed: 12418099]
15. Eliezer D. Biophysical characterization of intrinsically disordered proteins. Curr Opin Struct Biol. 2009; 19:23–30. [PubMed: 19162471]
16. Receveur-Bréchot V, Bourhis JM, Uversky VN, Canard B, Longhi S. Assessing protein disorder and induced folding. Proteins. 2006; 62:24–45. [PubMed: 16287116]
17. Kaltashov IA, Eyles SJ. Studies of biomolecular conformations and conformational dynamics by mass spectrometry. Mass Spectrom Rev. 2002; 21:37–71. [PubMed: 12210613]
18. Konermann L, Douglas DJ. Acid-Induced unfolding of cytochrome *c* at different methanol concentrations: Electrospray ionization mass spectrometry specifically monitors changes in the tertiary structure. Biochemistry. 1997; 36:12296–12302. [PubMed: 9315869]
19. Kaltashov IA, Abzalimov RR. Do ionic charges in ESI MS provide useful information on macromolecular structure? J Am Soc Mass Spectrom. 2008; 19:1239–1246. [PubMed: 18602274]
20. Konermann L, Douglas DJ. Equilibrium unfolding of proteins monitored by electrospray ionization mass spectrometry: distinguishing two-state from multi-state transitions. Rapid Commun Mass Spectrom. 1998; 12:435–442. [PubMed: 9586231]

21. Grandori R. Detecting equilibrium cytochrome c folding intermediates by electrospray ionisation mass spectrometry: Two partially folded forms populate the molten-globule state. Protein Sci. 2002; 11:453–458. [PubMed: 11847268]
22. Borysik AJ, Radford SE, Ashcroft AE. Co-populated conformational ensembles of β2-microglobulin uncovered quantitatively by electrospray ionization mass spectrometry. J Biol Chem. 2004; 279:27069–27077. [PubMed: 15100226]
23. Bobst CE, Abzalimov RR, Houde D, Kloczewiak M, Mhatre R, Berkowitz SA, Kaltashov IA. Detection and characterization of altered conformations of protein pharmaceuticals using complementary mass spectrometry-based approaches. Anal Chem. 2008; 80:7473–7481. [PubMed: 18729476]
24. Yu X, Wojciechowski M, Fenselau C. Assessment of metals in reconstituted metallothioneins by electrospray mass spectrometry. Anal Chem. 1993; 65:1355–1359. [PubMed: 8517548]
25. Gumerov DR, Kaltashov IA. Dynamics of iron release from transferrin N-lobe studied by electrospray ionization mass spectrometry. Anal Chem. 2001; 73:2565–2570. [PubMed: 11403301]
26. van den Bremer ET, Jiskoot W, James R, Moore GR, Kleanthous C, Heck AJ, Maier CS. Probing metal ion binding and conformational properties of the colicin E9 endonuclease by electrospray ionization time-of-flight mass spectrometry. Protein Sci. 2002; 11:1738–1752. [PubMed: 12070327]
27. Low LY, Hernandez H, Robinson CV, O'Brien R, Grossmann JG, Ladbury JE, Luisi B. Metal-dependent folding and stability of nuclear hormone receptor DNA-binding domains. J Mol Biol. 2002; 319:87–106. [PubMed: 12051939]
28. Griffith WP, Kaltashov IA. Highly asymmetric interactions between globin chains during hemoglobin assembly revealed by electrospray ionization mass spectrometry. Biochemistry. 2003; 42:10024–10033. [PubMed: 12924951]
29. Simmons DA, Wilson DJ, Lajoie GA, Doherty-Kirby A, Konermann L. Subunit disassembly and unfolding kinetics of hemoglobin studied by time-resolved electrospray mass spectrometry. Biochemistry. 2004; 43:14792–14801. [PubMed: 15544350]
30. Griffith WP, Kaltashov IA. Protein conformational heterogeneity as a binding catalyst: ESI-MS study of hemoglobin H formation. Biochemistry. 2007; 46:2020–2026. [PubMed: 17253776]
31. Kamadurai HB, Subramaniam S, Jones RB, Green-Church KB, Foster MP. Protein folding coupled to DNA binding in the catalytic domain of bacteriophage lambda integrase detected by mass spectrometry. Protein Sci. 2003; 12:620–626. [PubMed: 12592032]
32. Abzalimov RR, Dubin PL, Kaltashov IA. Glycosaminoglycans as naturally occurring combinatorial libraries: Developing a mass spectrometry-based strategy for characterization of anti-thrombin interaction with low molecular weight heparin and heparin oligomers. Anal Chem. 2007; 79:6055–6063. [PubMed: 17658885]
33. Lundvig D, Lindersson E, Jensen PH. Pathogenic effects of α-synuclein aggregation. Mol Brain Res. 2005; 134:3–17. [PubMed: 15790525]
34. Bennett MC. The role of α-synuclein in neurodegenerative diseases. Pharmacol Ther. 2005; 105:311–331. [PubMed: 15737408]
35. Cookson MR. The biochemistry of Parkinson's disease. Annu Rev Biochem. 2005; 74:29–52. [PubMed: 15952880]
36. Moore DJ, West AB, Dawson VL, Dawson TM. Molecular pathophysiology of Parkinson's disease. Annu Rev Neurosci. 2005; 28:57–87. [PubMed: 16022590]
37. Bonini NM, Giasson BI. Snaring the function of α-synuclein. Cell. 2005; 123:359–361. [PubMed: 16269324]
38. Uversky VN. A protein-chameleon: conformational plasticity of α-synuclein, a disordered protein involved in neurodegenerative disorders. J Biomol Struct Dyn. 2003; 21:211–234. [PubMed: 12956606]
39. Uversky VN, Yamin G, Souillac PO, Goers J, Glaser CB, Fink AL. Methionine oxidation inhibits fibrillation of human α-synuclein in vitro. FEBS Lett. 2002; 517:239–244. [PubMed: 12062445]

40. Mohimen A, Dobo A, Hoerner JK, Kaltashov IA. A chemometric approach to detection and characterization of multiple protein conformers in solution using electrospray ionization mass spectrometry. Anal Chem. 2003; 75:4139–4147. [PubMed: 14632127]
41. Konermann L. A minimalist model for exploring conformational effects on the electrospray charge state distribution of proteins. J Phys Chem B. 2007; 111:6534–6543. [PubMed: 17511498]
42. Kaltashov IA, Mohimen A. Estimates of protein surface areas in solution by electrospray ionization mass spectrometry. Anal Chem. 2005; 77:5370–5379. [PubMed: 16097782]
43. Felitsyn N, Kitova EN, Klassen JS. Thermal dissociation of the protein homodimer ecotin in the gas phase. J Am Soc Mass Spectrom. 2002; 13:1432–1442. [PubMed: 12484463]
44. Abzalimov RR, Frimpong AK, Kaltashov IA. Gas-phase processes and measurements of macromolecular properties in solution: On the possibility of false positive and false negative signals of protein unfolding. Int J Mass Spectrom. 2006; 253:207–216.
45. Le Gall T, Romero PR, Cortese MS, Uversky VN, Dunker AK. Intrinsic disorder in the Protein Data Bank. J Biomol Struct Dyn. 2007; 24:325–342. [PubMed: 17206849]
46. Koo EH, Lansbury PT Jr, Kelly JW. Amyloid diseases: Abnormal protein aggregation in neurodegeneration. Proc Natl Acad Sci U S A. 1999; 96:9989–9990. [PubMed: 10468546]
47. Thompson AJ, Barrow CJ. Protein conformational misfolding and amyloid formation: characteristics of a new class of disorders that include Alzheimer's and Prion diseases. Curr Med Chem. 2002; 9:1751–1762. [PubMed: 12369885]
48. Dobson CM. Protein aggregation and its consequences for human disease. Protein Pept Lett. 2006; 13:219–227. [PubMed: 16515449]
49. Uversky VN, Oldfield CJ, Dunker AK. Intrinsically Disordered Proteins in Human Diseases: Introducing the D2 Concept. Annual Review of Biophysics. 2008; 37:215–246.
50. Johnson WG. Late-onset neurodegenerative diseases - the role of protein insolubility. J Anat. 2000; 196:609–616. [PubMed: 10923991]
51. Trojanowski JQ, Lee VMY. Parkinson's disease and related synucleinopathies are a new class of nervous system amyloidoses. NeuroToxicology. 2002; 23:457–460. [PubMed: 12428717]
52. Lee JC, Lai BT, Kozak JJ, Gray HB, Winkler JR. α-Synuclein tertiary contact dynamics. J Phys Chem B. 2007; 111:2107–2112. [PubMed: 17279794]
53. Ly T, Julian RR. Protein-metal interactions of calmodulin and α-synuclein monitored by selective noncovalent adduct protein probing mass spectrometry. J Am Soc Mass Spectrom. 2008; 19:1663–1672. [PubMed: 18691903]
54. Ulmer TS, Bax A, Cole NB, Nussbaum RL. Structure and dynamics of micelle-bound human α-synuclein. J Biol Chem. 2005; 280:9595–9603. [PubMed: 15615727]
55. Ferreon ACM, Deniz AA. α-Synuclein multistate folding thermodynamics: implications for protein misfolding and aggregation. Biochemistry. 2007; 46:4499–4509. [PubMed: 17378587]
56. Kuprowski MC, Konermann L. Signal response of coexisting protein conformers in electrospray mass spectrometry. Anal Chem. 2007; 79:2499–2506. [PubMed: 17288464]
57. Dobo A, Kaltashov IA. Detection of multiple protein conformational ensembles in solution via deconvolution of charge state distributions in ESI MS. Anal Chem. 2001; 73:4763–4773. [PubMed: 11681449]
58. Frimpong AK, Abzalimov RR, Eyles SJ, Kaltashov IA. Gas-phase interference-free analysis of protein ion charge-state distributions: detection of small-scale conformational transitions accompanying pepsin inactivation. Anal Chem. 2007; 79:4154–4161. [PubMed: 17477507]
59. Grabenauer M, Bernstein SL, Lee JC, Wyttenbach T, Dupuis NF, Gray HB, Winkler JR, Bowers MT. Spermine binding to Parkinson's protein α-synuclein and its disease-related A30P and A53T mutants. J Phys Chem B. 2008; 112:11147–11154. [PubMed: 18693700]
60. Bernstein SL, Liu D, Wyttenbach T, Bowers MT, Lee JC, Gray HB, Winkler JR. α-Synuclein: stable compact and extended monomeric structures and pH dependence of dimer formation. J Am Soc Mass Spectrom. 2004; 15:1435–1443. [PubMed: 15465356]
61. Sharon M, Robinson CV. The role of mass spectrometry in structure elucidation of dynamic protein complexes. Annu Rev Biochem. 2007; 76:167–193. [PubMed: 17328674]

62. Maiti NC, Apetri MM, Zagorski MG, Carey PR, Anderson VE. Raman spectroscopic characterization of secondary structure in natively unfolded proteins: α-synuclein. J Am Chem Soc. 2004; 126:2399–2408. [PubMed: 14982446]

63. Del Mar C, Greenbaum EA, Mayne L, Englander SW, Woods VL Jr. Structure and properties of α-synuclein and other amyloids determined at the amino acid level. Proc Natl Acad Sci U S A. 2005; 102:15477–15482. [PubMed: 16223878]

64. Jurchen JC, Garcia DE, Williams ER. Further studies on the origins of asymmetric charge partitioning in protein homodimers. J Am Soc Mass Spectrom. 2004; 15:1408–1415. [PubMed: 15465353]

65. Fink AL. The aggregation and fibrillation of α-synuclein. Acc Chem Res. 2006; 39:628–634. [PubMed: 16981679]

66. Apetri MM, Maiti NC, Zagorski MG, Carey PR, Anderson VE. Secondary structure of α-synuclein oligomers: Characterization by Raman and atomic force microscopy. J Mol Biol. 2006; 355:63–71. [PubMed: 16303137]

67. Dusa A, Kaylor J, Edridge S, Bodner N, Hong DP, Fink AL. Characterization of oligomers during α-synuclein aggregation using intrinsic tryptophan fluorescence. Biochemistry. 2006; 45:2752–2760. [PubMed: 16489768]

68. Heck AJR. Native mass spectrometry: a bridge between interactomics and structural biology. Nat Meth. 2008; 5:927–933.

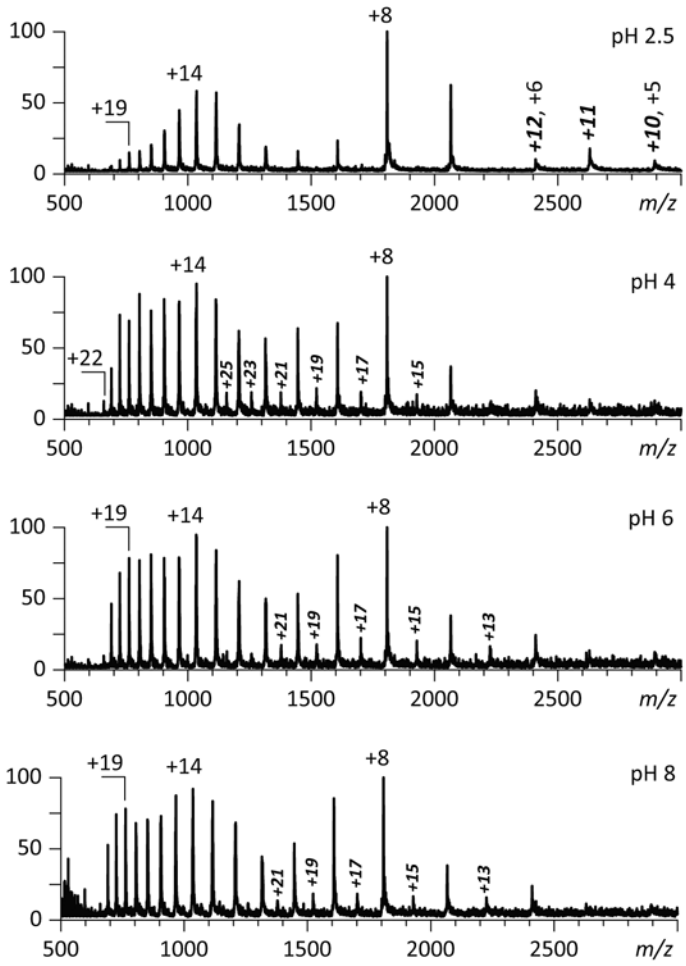

Figure 1.

ESI mass spectra of α-synuclein acquired in the pH range 2.5 to 8 (protein concentration 10 μM). Charge states of monomeric protein ions are indicated on the graphs (normal type). Numbers in bold italics indicate charge states of non-covalently bound protein dimer ions.

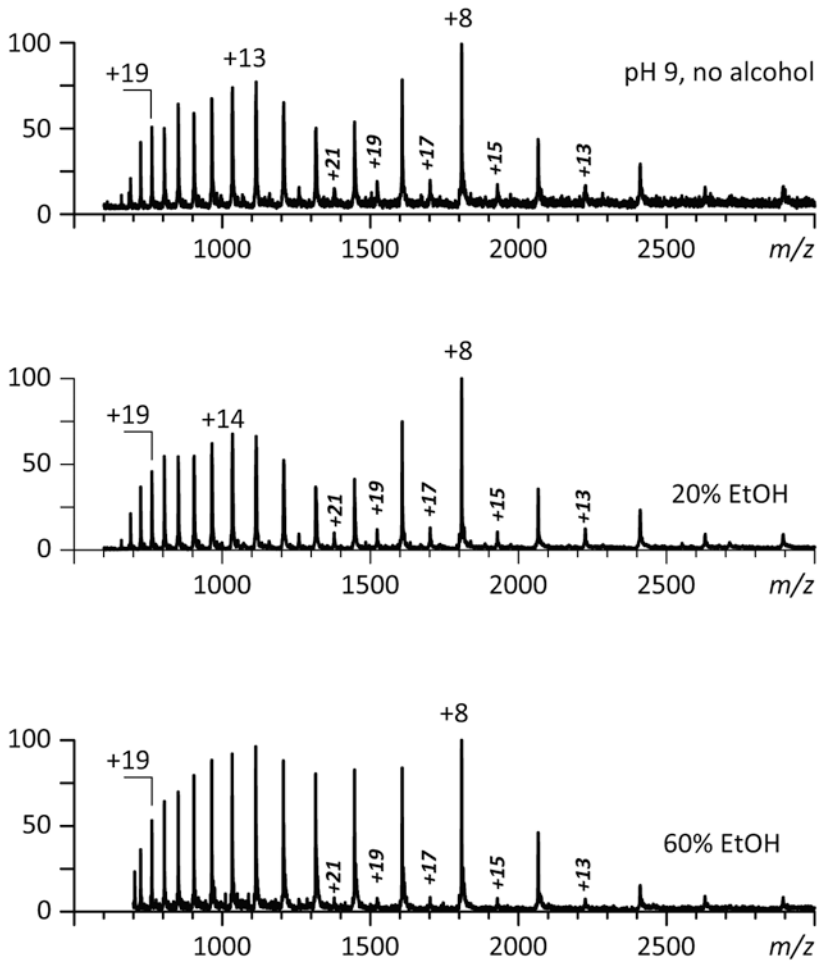

Figure 2.

ESI mass spectra of α-synuclein acquired at pH 9 in the absence and in the presence of ethanol and TFE as co-solvents (protein concentration 10 μM). Charge states of monomeric protein ions are indicated with the normal type numbers and those of non-covalently bound protein dimers are in bold italics.

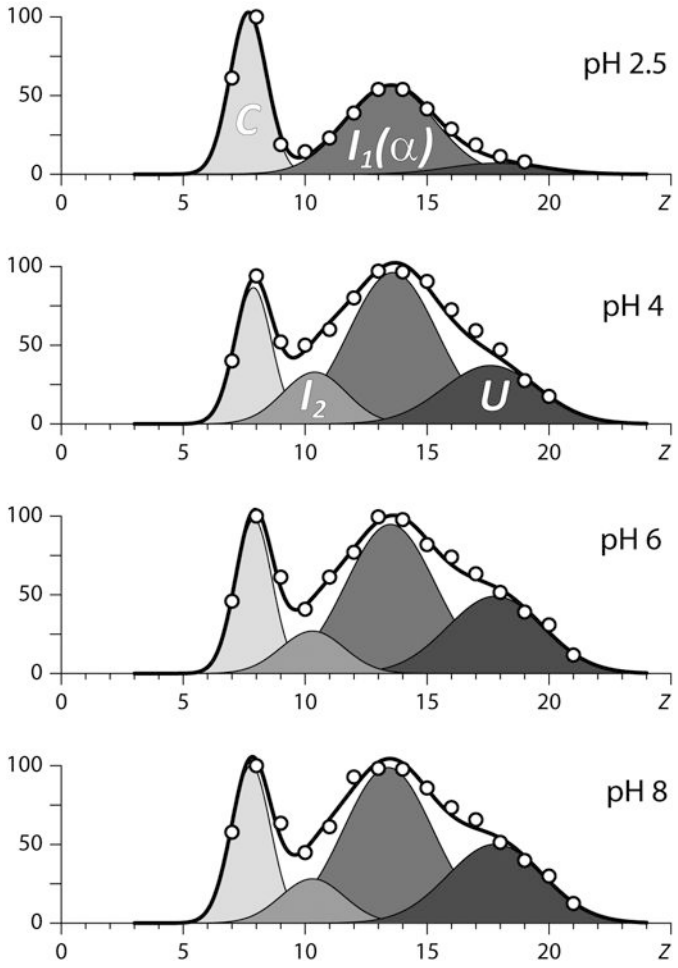

Figure 3.

The results of deconvolution of charge state distributions of α-synuclein ions in ESI MS acquired in the pH range 2.5 to 8 (the raw data are presented in Figure 1). The four basis functions are assigned to the following putative states of the protein (from darker to lighter shade of gray): ***U***, unstructured; $\boldsymbol{I}_1$, helix-rich intermediate state; $\boldsymbol{I}_2$, β-sheet-rich intermediate state; and ***C***, highly compact.

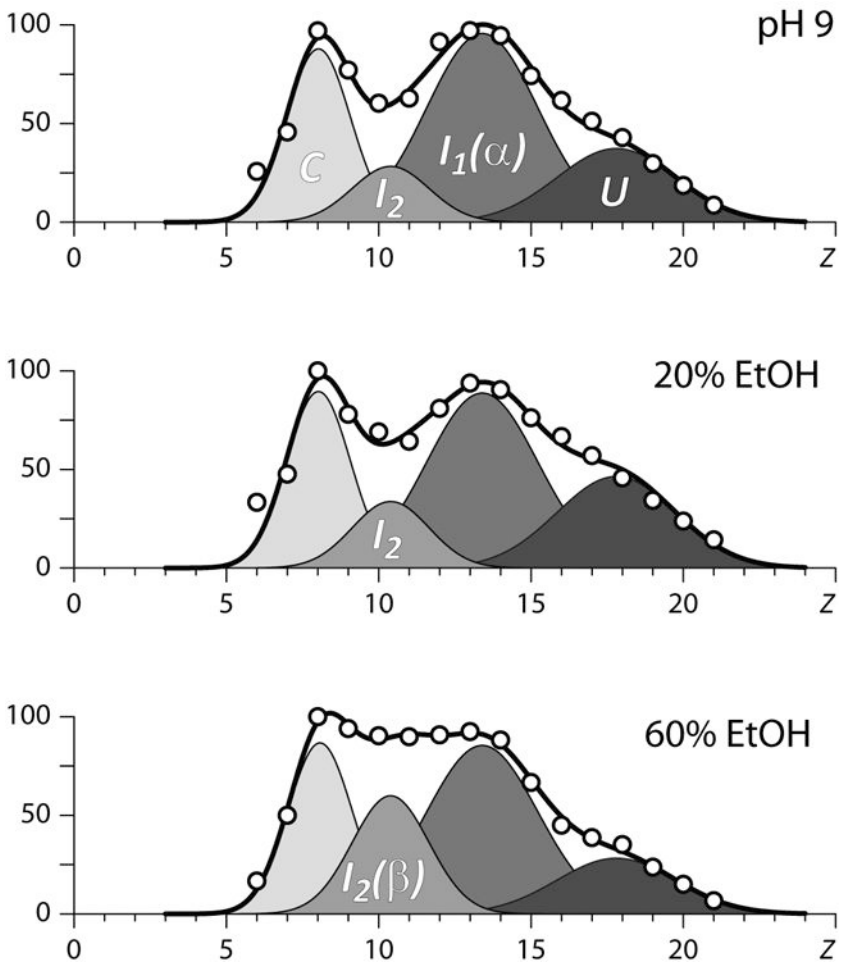

Figure 4.

The results of deconvolution of charge state distributions of α-synuclein ions in ESI MS acquired at pH 9 in the absence of alcohol (top diagram) and in the presence of ethanol (20% by volume, middle, and 60% by volume, bottom). The raw data are presented in Figure 2. The four basis functions are assigned to the following putative states of the protein (from darker to lighter shade of gray): ***U***, unstructured; $\boldsymbol{I}_1$, helix-rich intermediate state; $\boldsymbol{I}_2$, β-sheet-rich intermediate state; and ***C***, highly compact.

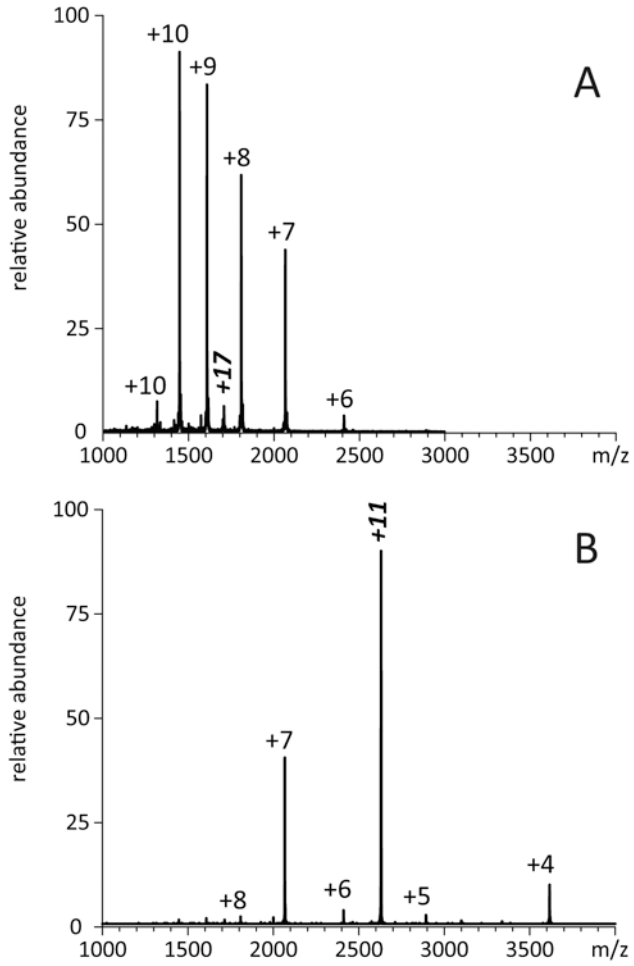

Figure 5.

Fragmentation mass spectra of α-synuclein dimer ions generated by ESI MS at pH 8.0 (**A**) and 2.5 (**B**). Precursor ions are labeled in bold italics; charge states of fragment ions (monomers) are labeled in normal type.

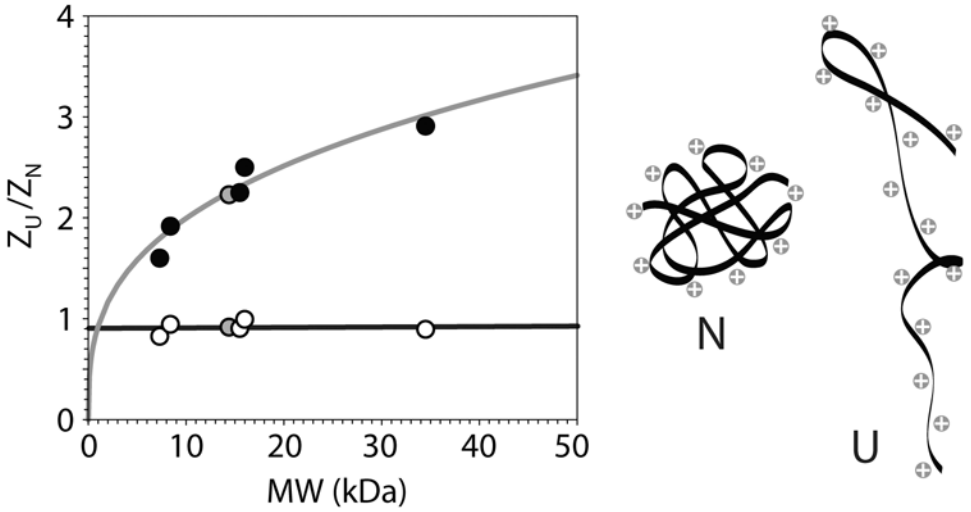

Figure 6.

Ratio of average charges accommodated by random coils ($Z_{\mathbf{U}}$) and natively folded proteins ($Z_{\mathbf{N}}$) as a function of protein mass (filled circles) and values of $Z_{\mathbf{U}}/Z_{\mathbf{N}}$ normalized to $\sqrt[3]{\text{MW}}$ (open circles). The shaded data point corresponds to α-synuclein. Other proteins represented in this graph (listed in order of increasing MW) are: chymotrypsin inhibitor 2, ubiquitin, CRABP I, myoglobin, and pepsin.